Fortschr. Phys. **51**, No. 2–3, 157 – 171 (2003) / **DOI** 10.1002/prop.200310020

Two-mode Schrödinger cats, entanglement and teleportation

J. Janszky[1,*], **J. Asbóth**[1], **A. Gábris**[1], **A. Vukics**[1], **M. Koniorczyk**[1,2], and **T. Kobayashi** [3]

[1] Research Institute for Solid State Physics and Optics, Hungarian Academy of Sciences, P.O. Box 49, 1525 Budapest, Hungary

[2] Institute of Physics, University of Pécs, Ifjúság út 6, 7624 Pécs, Hungary

[3] Department of Physics, University of Tokyo, 7-3-1 Hongo, Bunkyo-ku, Tokyo, Japan

Received 10 June 2002, accepted 19 June 2002
Published online 25 February 2003

Two-mode Schrödinger cats consisting of two and four coherent-state terms are considered. It is shown that they are closely related to the quadrature entangled EPR pair. The properties of their wave functions are investigated from their aspects of entanglement. It is shown that at certain parameters the entangled properties of the two-mode Schrödinger cats allow for good teleportation fidelity. A theoretical generalization to the teleportation of two qubits is also discussed.

1 Introduction

A Schrödinger cat (SC) is a coherent superposition of macroscopically distinguishable quantum states. In quantum optics the macroscopically different quantum states are usually coherent states of a mode of light. Even and odd Schrödinger cats ($|\alpha,+\rangle$, $|\alpha,-\rangle$) are then defined as follows:

$$|\alpha,\pm\rangle := N_{|\alpha,\pm\rangle}(|\alpha\rangle \pm |-\alpha\rangle), \tag{1}$$

where $N_{|\alpha,\pm\rangle} = (2 \pm 2\exp(-2|\alpha|^2))^{-1/2}$ is the normalization factor. Schrödinger cats exhibit various nonclassical features, e.g. squeezing, sub-Poissonian statistics, oscillations in photon number, due to quantum interference between the composite coherent states.

The concept of Schrödinger cats can be generalized to two-mode states in many ways [1–3]. In the following we are going to examine a two-mode *entangled* Schrödinger cat state defined as

$$|g,2\pm\rangle := N_{|g,2\pm\rangle}(|g^*,g\rangle \pm |g,g^*\rangle + |-g^*,-g\rangle \pm |-g,-g^*\rangle), \tag{2}$$
$$\text{where } N_{|g,2\pm\rangle} = \frac{1}{2\sqrt{2}} e^{|g|^2} / \sqrt{\cosh(2|g^2|) \pm \cosh(2\mathbf{Re}(g^2))}$$

is a normalization factor. Here g is a complex number, and $|\alpha,\beta\rangle$ denotes a two-mode coherent state. In the special case where the amplitude g is real, the state $|g,2+\rangle$ becomes the even two-mode coherent state $|g,g\rangle + |-g,-g\rangle$ of [2], if g is imaginary, $|g,2+\rangle$ becomes $|g,-g\rangle + |-g,g\rangle$, a two-mode entangled coherent state considered in [4]. If g is real or imaginary, $|g,2-\rangle$ is nonphysical (has zero norm), but the limits $\mathbf{Im}g \to 0$, $\mathbf{Re}g \to 0$ are well defined, and lead to two-mode entangled states.

The main motivation for choosing this form of the two-mode Schrödinger cat is that it is easily generated from one-mode Schrödinger cats with a beam splitter. Let us take a beam splitter that in the Heisenberg picture acts on the annihilation operators of the modes in the following way:

* Corresponding author E-mail: janszky@szfki.hu

 0015-8208/03/2–302-0157 $ 17.50+.50/0

$$\begin{pmatrix} \hat{a}' \\ \hat{b}' \end{pmatrix} = \frac{1}{\sqrt{2}} \begin{pmatrix} 1 & 1 \\ -1 & 1 \end{pmatrix} \begin{pmatrix} \hat{a} \\ \hat{b} \end{pmatrix},$$

where $\hat{a}$,$\hat{b}$, and $\hat{a}'$,$\hat{b}'$ are the annihilation operators of the input and output modes respectively. If two coherent states $|q_0\rangle\,, |ip_0\rangle$ enter the beam splitter at the input modes, two coherent states constituting a two-mode coherent state appear at the output modes:

$$|q_0\rangle \otimes |ip_0\rangle \longrightarrow \left| \frac{q_0 - ip_0}{\sqrt{2}}, \frac{q_0 + ip_0}{\sqrt{2}} \right\rangle . \tag{3}$$

If the input states are one-mode Schrödinger cat states, and not one-mode coherent states, the state leaving the beam splitter can be calculated:

$$\begin{aligned} &N_{|q_0,\pm\rangle} \left(|q_0\rangle \pm |-q_0\rangle\right) \otimes N_{|ip_0,\pm\rangle} \left(|ip_0\rangle \pm |-ip_0\rangle\right) \rightarrow \\ &\quad N_{|g,2\pm\rangle} \left(|g^*, g\rangle \pm |g, g^*\rangle + |-g^*, -g\rangle \pm |-g, -g^*\rangle\right), \end{aligned} \tag{4}$$

where q_0 and p_0 are chosen to be real and $g = \frac{q_0+ip_0}{\sqrt{2}}$. It can thus be seen that two even (odd) Schrödinger cats interacting on a $50:50$ real beam splitter give the state $|g, 2+\rangle$ ($|g, 2-\rangle$).

2 Photon number statistics, quadrature wavefunctions, time evolution

Let us consider the photon number distribution of the states $|g, 2\pm\rangle$ in each mode. Using the number-state expansion of a two-mode coherent state:

$$|\alpha, \beta\rangle = \mathrm{e}^{-(|\alpha|^2+|\beta|^2)/2} \sum_{n=0}^{\infty} \sum_{m=0}^{\infty} \frac{\alpha^n \beta^m}{\sqrt{n!m!}} |n, m\rangle\,, \tag{5}$$

the expansion of $|g, 2\pm\rangle$ is easily calculated:

$$\begin{aligned} |g, 2\pm\rangle \;&=\; N_{|g,2\pm\rangle} e^{-|g|^2} \sum_{n,m=0}^{\infty} \frac{2|g|^{2\min(n,m)}}{\sqrt{n!m!}} ((n+m+1) \bmod 2)\; c^{\pm}_{nm} |n, m\rangle\,, \\ c^{+}_{nm} \;&=\; \mathbf{Re}(g^{|n-m|}), \\ c^{-}_{nm} \;&=\; \mathrm{sign}(n-m)\; \mathbf{Im}(g^{|n-m|}). \end{aligned} \tag{6}$$

We immediately see that the total number of photons in the two modes cannot be odd, therefore these states can be considered as generalizations of the "even coherent state" of [2]. Moreover, if the argument of the complex coherent amplitude parameter g is a rational multiple of π, further zero coefficients appear in the photon number distribution. The number of these additional zeros is highest if this angle is $\pi/4$, i.e. $\mathbf{Re}g = \mathbf{Im}g$, in that case only 25% of the Fock state components have nonzero amplitude.

The photon number distribution of the even two-mode SC state $|g, 2+\rangle$ is symmetrical with respect to the swapping of the two modes, whereas that of $|g, 2-\rangle$ is antisymmetrical. Moreover, for the even two-mode SC state the symmetrical Fock states ($n = m$) have high probability amplitudes, whereas the odd SC state has no symmetrical Fock state component. An interesting consequence of this is that if we examine two-mode SCs of less and less energy (we let $g \to 0$ in some well defined way), for the even SC we always end up with the two-mode vacuum $|0, 0\rangle$, whereas for the odd SC a superposition of two Fock-states: $1/\sqrt{2}(|0, 2\rangle - |2, 0\rangle)$ is reached. In the generation scheme introduced in section 1, the above limit means that the amplitudes of the one-mode Schrödinger cats that make up $|g, 2\pm\rangle$ tend to zero. In the case of the even one-mode SC the state reached at the limit is the vacuum, whereas for the odd SC it is the Fock state $|1\rangle$. Two vacua impinging on a beam splitter yield the two-mode vacuum at the output ports, whereas two $|1\rangle$ states yield $1/\sqrt{2}(|0, 2\rangle - |2, 0\rangle)$. The latter state has nonzero entanglement, which indicates that odd two-mode SC states with small amplitudes can be useful for quantum teleportation.

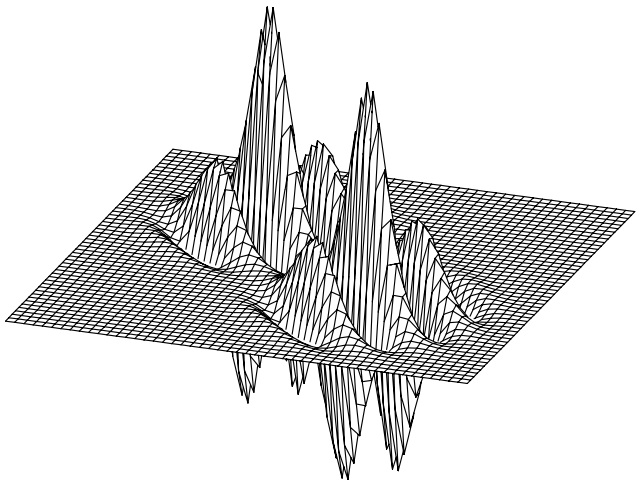

Fig. 1 The quadrature wavefunction of $|g, 2\pm\rangle$ at $q_0 = 2, p_0 = 3$.

The mean photon number of the $|g, 2\pm\rangle$ states is an important quantity, since it is related to their mean energy:

$$\langle g, 2\pm| \hat{a}^+\hat{a} + \hat{b}^+\hat{b} |g, 2\pm\rangle = \frac{2|g^2| \sinh\left(2|g^2|\right) \pm 2\mathbf{Re}\left(g^2\right) \sinh\left(2\mathbf{Re}\left(g^2\right)\right)}{\cosh\left(2|g^2|\right) \pm \cosh\left(2\mathbf{Re}\left(g^2\right)\right)}. \tag{7}$$

A useful tool for the description of the $|g, 2\pm\rangle$ states is their (time-dependent) quadrature wave function. This is just the sum of the quadrature wavefunctions of the component two-mode coherent states. Denoting the quadratures by q_1 and q_2 we have:

$$\begin{aligned} \Psi_+(q_1, q_2) = &\quad N_+ \mathrm{e}^{-\frac{q_1^2+q_2^2}{2}} \cos\left(\left(q_1 - q_2\right) p_0 \mathrm{e}^{-\mathrm{i}\omega t}\right) \cosh\left(\left(q_1 + q_2\right) q_0 \mathrm{e}^{-\mathrm{i}\omega t}\right), \\ \Psi_-(q_1, q_2) = &\quad N_- \mathrm{e}^{-\frac{q_1^2+q_2^2}{2}} i \sin\left(\left(q_1 - q_2\right) p_0 \mathrm{e}^{-\mathrm{i}\omega t}\right) \sinh\left(\left(q_1 + q_2\right) q_0 \mathrm{e}^{-\mathrm{i}\omega t}\right), \end{aligned} \tag{8}$$

where the upper and lower rows are the wave functions of the even and odd two-mode Schrödinger cats, respectively. The normalizing factors $N_\pm$ are given by:

$$N_\pm = \sqrt{\frac{2}{\pi}} \frac{\exp\left(\frac{q_0^2+p_0^2}{2} - \mathrm{e}^{-\mathrm{i}\omega t}\left(q_0^2 \cos(\omega t) + i p_0^2 \sin(\omega t)\right)\right)}{\sqrt{\cosh\left(q_0^2 + p_0^2\right) \pm \cosh\left(q_0^2 - p_0^2\right)}}. \tag{9}$$

These wavefunctions are completely real (completely imaginary) at $t = 0$, so they can be plotted as 3-dimensional curved surfaces. A typical example (for $q_0 2, p_0 = 3$) is shown on Fig. 1. At $t \neq 0$, however, the wave functions are complex valued, and therefore cannot be represented in such a simple way. We can follow the time evolution of the states through the joint quadrature probability density. The probability density for finding a given pair of quadratures (q_1, q_2) is:

$$\begin{aligned} \rho_{|4\pm\rangle}(q_1, q_2) &= \Psi_{|g,2\pm\rangle}(q_1, q_2)^* \Psi_{|g,2\pm\rangle}(q_1, q_2) \\ &= \pm\frac{1}{2\pi} \frac{\exp\left(q_0^2 + p_0^2 - 2\left(q_0^2 \cos^2(\omega t) + p_0^2 sin^2(\omega t)\right)\right)}{\cosh\left(q_0^2 + p_0^2\right) \pm \cosh\left(q_0^2 - p_0^2\right)} \\ &\quad \mathrm{e}^{-\left(q_1^2+q_2^2\right)} \{\cosh(2q_0(q_1 + q_2)\cos(\omega t)) \pm \cos\left(2q_0(q_1 + q_2)\sin(\omega t)\right)\} \\ &\quad \{\cosh\left(2p_0(q_1 - q_2)\sin(\omega t)\right) \pm \cos\left(2p_0(q_1 - q_2)\cos(\omega t)\right)\}. \end{aligned} \tag{10}$$

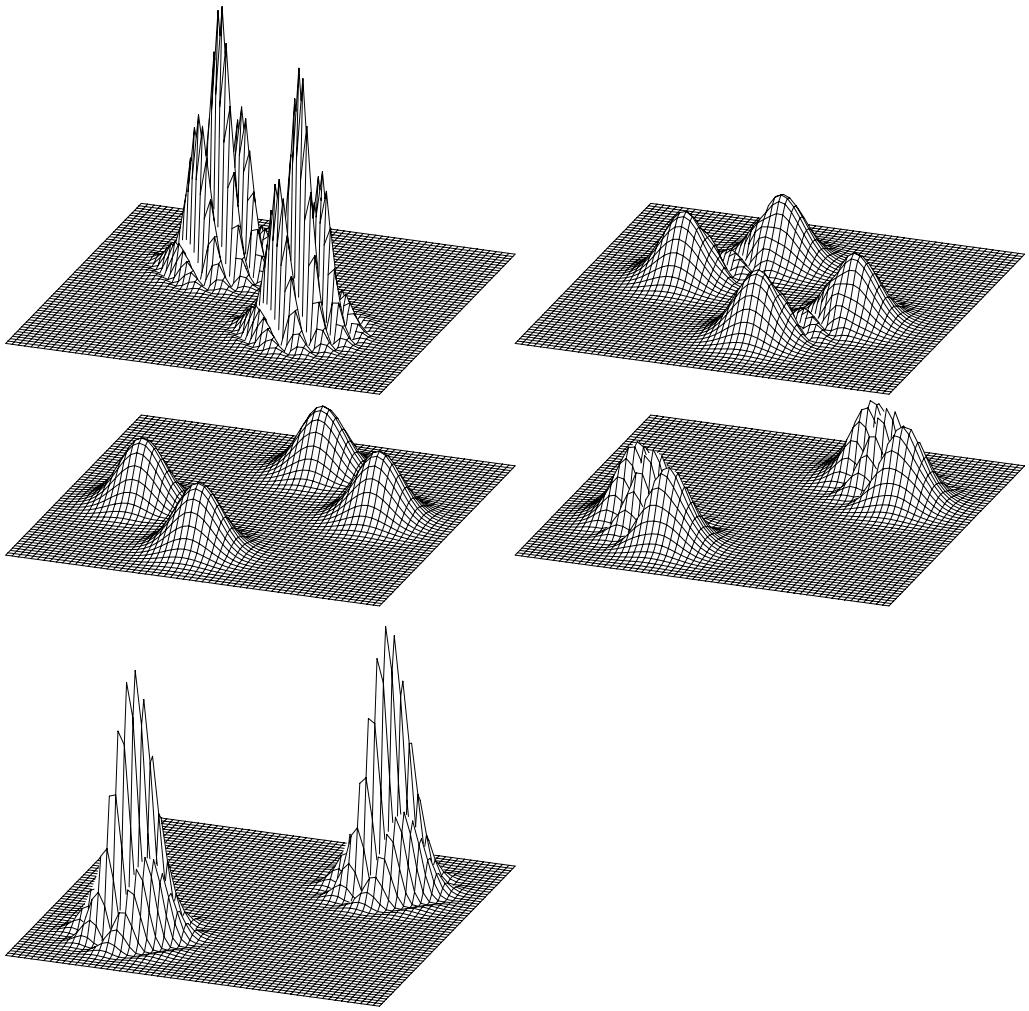

Fig. 2 The time evolution of the joint quadrature probability density function of the state $|2+3i, 2+\rangle$ is shown from $t = 0$ to $t = T/2$ as a typical example of the two-mode Schrödinger cat states. The pictures from top left to bottom correspond to $t = 0, t = T/8, t = T/4, t = 3T/8, t = T/2$.

The time evolution of the quadrature probability density function is shown in Fig. 2. Four humps can be observed in the quadrature probability density function, two of them rotating clockwise and two anticlockwise with period T around the origin on an elliptical trajectory. At $t = kT/2$ the humps collide at the endpoints of one of the diameters of the ellipse. These endpoints are situated at $(q_0, q_0), (-q_0, -q_0)$ for $t = kT$, and $(-p_0, p_0), (p_0, -p_0)$ for $t = kT + T/2$. At the collision times only two humps are seen, with ripples over them in the direction perpendicular to the line connecting them, the number of waves over the humps corresponds to the length of the other diagonal of the ellipse.

The difference between the $|g, 2+\rangle$ and $|g, 2-\rangle$ states is seen at the collision times: the first have one hump over each endpoint of the diagonal, the latter two humps.

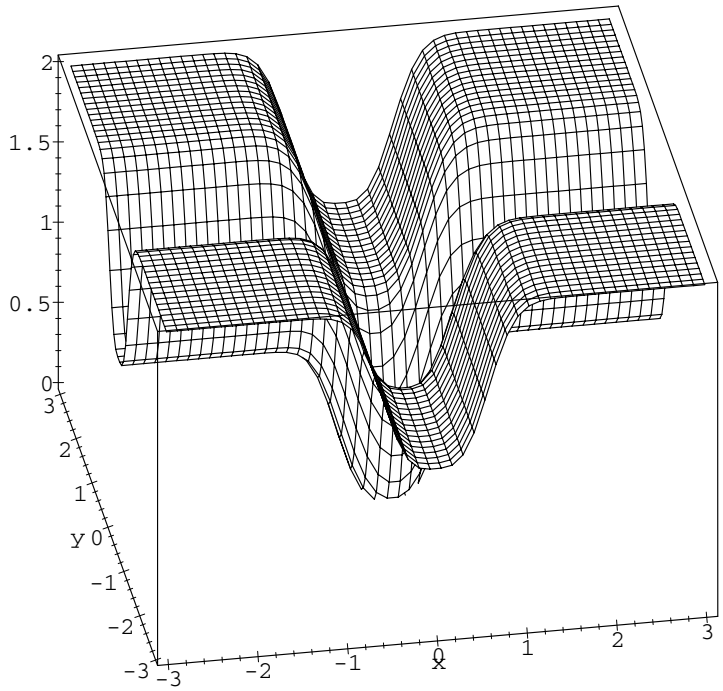

Fig. 3 The entanglement of even two-mode Schrödinger cat states $|g, 2+\rangle$ are plotted as a function of their coherent amplitude parameter g. If both $\mathbf{Re}g$ and $\mathbf{Im}g$ have large values, the state has two ebits of entanglement, since in that case the component coherent states are almost orthogonal. Both $\mathbf{Re}g$ and $\mathbf{Im}g$ may contribute to 1 ebit: if either of them is smaller than 1, the entanglement is reduced, approaching 1 ebit when either $\mathbf{Re}g$ or $\mathbf{Im}g$ is 0, the other one is large, and 0 when both of them are very small. In this latter case the state is very similar to the two-mode vacuum.

3 Entanglement

The entanglement of a pure bipartite quantum state is generally quantified by the *information content of entanglement* [5], the von Neumann entropy of either of its subsystems viewed independently of the other:

$$E(\Psi) = S(\hat{\varrho}^{(a)}) = -\operatorname{tr} \hat{\varrho}^{(a)} \log \hat{\varrho}^{(a)}. \tag{11}$$

Here $\hat{\varrho}^{(a)} = \operatorname{tr}_b |\Psi\rangle \langle\Psi|$ is the reduced density matrix obtained by tracing the whole system's pure-state density matrix over the degrees of freedom of the subsystem b.

For the evaluation of the above entropy we need to calculate the eigenvalues of the reduced density matrix $\hat{\varrho}^{(a)}$. Using the Fock basis the matrix representing $\varrho^{(a)}$ is $\infty \times \infty$. The four nonzero eigenvalues of this matrix could then be calculated approximately e.g. by suitable iterative truncations of the matrix (ignoring Fock states with number of particles very large). Although this calculation is feasible, it only leads to approximate formulae. To examine the behaviour of the entanglement in the parameter space, the whole procedure would have to be repeated for many parameter values.

Using a suitable *non-orthogonal* base, where the basis vectors are $|g\rangle, |g^*\rangle, |-g\rangle, |-g^*\rangle$, for the representation of the reduced density matrix $\hat{\varrho}^{(a)}$, the calculation can be solved much more effectively. Introducing the metric tensor, as described in the Appendix, all we need to calculate are the eigenvalues of a 4×4 matrix. This not only takes shorter time, but can even be done analytically, thereby allowing the exploration of the parameter space with arbitrary precision. Since the exact formulae are long, and not very instructive, we omit them, and present plots of the entanglement on Figs. 3, 4.

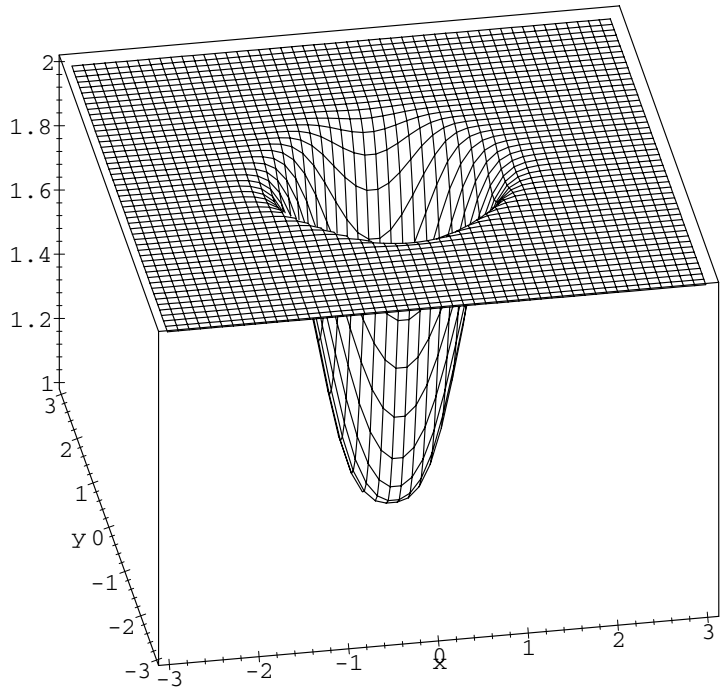

Fig. 4 The entanglement of odd two-mode Schrödinger cat states $|g, 2-\rangle$ are plotted as a function of their coherent amplitude parameter g. If $|g| > 1$, the state has approximately two ebits of entanglement. In the limit $|g| \to 0$, the entanglement becomes 1 ebit, since in that case the state $|0, 2\rangle + |2, 0\rangle$ is reached.

4 Two-mode Schrödinger cat and two-mode squeezed vacuum

Squeezed states have been the subject of intensive research in the recent years. One such state is the amplitude squeezed vacuum state,

$$|SqV\rangle = \hat{S}(\zeta)\,|0\rangle\,, \quad \hat{S}(\zeta) = \mathrm{e}^{\frac{\zeta^*}{2}\hat{a}\hat{a} - \frac{\zeta}{2}\hat{a}^+\hat{a}^+}. \tag{12}$$

Amplitude squeezed vacuum states have minimum uncertainty in their quadratures, furthermore, all minimum-uncertainty states are displaced amplitude squeezed vacua.

If two oppositely squeezed vacua interfere on a 50:50 real beam-splitter, they produce a two-mode squeezed vacuum. This is the strongest entangled state possible with given mean energy, and it provides a physical realization of the original Einstein-Podolsky-Rosen state. It can be constructed from two mode vacuum with the two-mode squeezing operator $\hat{S}^{(2)}$:

$$|2SqV\rangle = \hat{S}^{(2)}(r)\,|0,0\rangle\,, \quad \hat{S}^{(2)}(r) = \mathrm{e}^{r^*\hat{a}\hat{b} - r\hat{a}^+\hat{b}^+}. \tag{13}$$

For suitably chosen, small values of g and r, our $|g, 2\pm\rangle$ state becomes very similar to the two-mode squeezed vacuum. This similarity, apparent from their wavefunctions, can be quantified by the overlap of the two states. The overlap is calculated using the factorized form of the two-mode squeezing operator found in [6]:

$$\hat{S}^{(2)}\,(r) = \frac{1}{\cosh|r|}\mathrm{e}^{-\mathrm{e}^{\mathrm{i}\Phi}\tanh|r|\hat{a}^+\hat{b}^+}\mathrm{e}^{\ln\cosh|r|\left(\hat{a}^+\hat{a}+\hat{b}^+\hat{b}\right)}\mathrm{e}^{-\mathrm{e}^{-\mathrm{i}\Phi}\tanh|r|\hat{a}\hat{b}}. \tag{14}$$

Acting with this operator on the two-mode vacuum, the third and second factors simplify to unity.

$$|2SqV\rangle = \frac{1}{\cosh|r|}\exp(-\mathrm{e}^{\mathrm{i}\Phi}\tanh|r|\hat{a}^{+}\hat{b}^{+})\,|0,0\rangle\,. \tag{15}$$

Using this formula, the overlap of the two-mode squeezed vacuum and a two-mode coherent state $|g,h\rangle$ can be easily calculated by letting the creation operators in the exponent of (15) act on the bra vector:

$$\langle g,h|\,2SqV\rangle = \frac{\exp(-g^{*}h^{*}\mathrm{e}^{\mathrm{i}\Phi}\tanh|r|)}{\cosh r}\mathrm{e}^{-\frac{|g|^2}{2}-\frac{|h|^2}{2}}. \tag{16}$$

This gives $\langle g,2-|\,2SqV\rangle = 0$, as expected from the symmetry properties of these states, and

$$\begin{aligned}\langle g,2+|\,2SqV\rangle &= 4C_{|g,2\pm\rangle}\frac{\exp(-|g|^2(\mathrm{e}^{\mathrm{i}\Phi}\tanh|r|+1))}{\cosh|r|}\\ &= \frac{\sqrt{2}}{\cosh|r|}\frac{\exp(-|g|^2\mathrm{e}^{\mathrm{i}\Phi}\tanh|r|)}{\sqrt{\cosh(2|g^2|)+\cosh(2\mathbf{Re}\,(g^2))}}.\end{aligned} \tag{17}$$

The difference of the two states is quantified by one minus the squared modulus of their overlap. In the simple case of $\Phi=\pi$ and $p_0=q_0$ this is:

$$1-|\,\langle g,2+|\,2SqV\rangle\,|^2 = 1-\frac{2}{\cosh^2|r|}\quad\frac{\mathrm{e}^{2q_0^2\tanh r}}{\cosh(2q_0^2)+1}. \tag{18}$$

The overlap of these two states, and their difference for small values of r and q_0 is plotted in Fig. 5. It can be seen that the difference of the two states is less than 10^{-5} for suitable, small values of r and q_0.

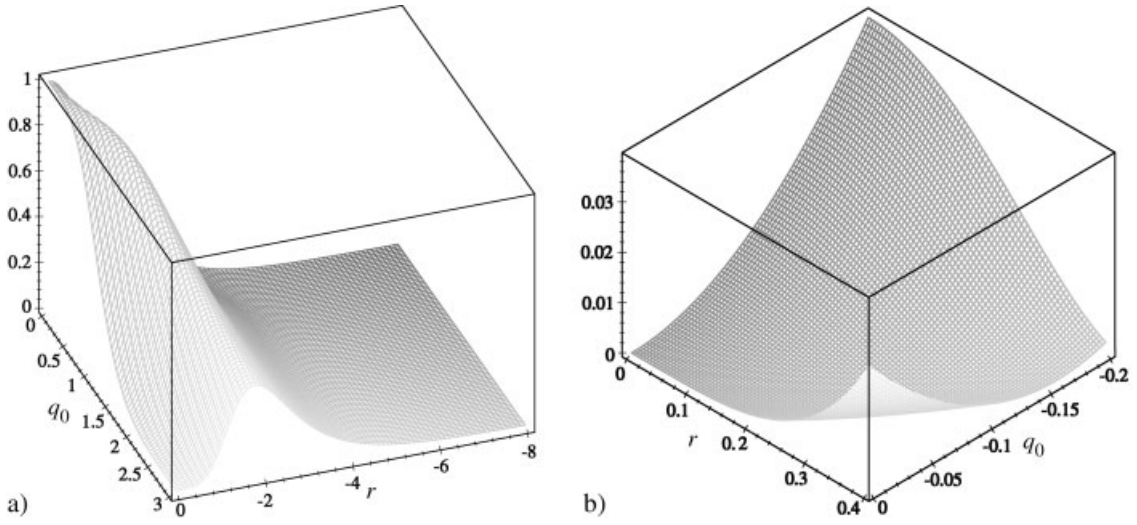

Fig. 5 The overlap and difference of the two-mode squeezed vacuum and $|g,2\pm\rangle$. In the upper figure the overlap of the two-mode squeezed vacuum with negative real squeezing parameter r, and the $|g,2\pm\rangle$ state with $p_0=q_0$ is shown as function of their parameters. In the lower figure the physically more interesting quantity, their difference is plotted for small values of r and q_0. As seen from the figure, this difference is below 10^{-5} for suitably chosen parameters.

5 Teleportation by Schrödinger cats

As an example of application of two-mode Schrödinger cats as an entangled resource we consider a scheme for *conditional* teleportation of the state

$$|\Psi_{\text{in}}\rangle = \gamma_0 |0\rangle + \gamma_1 |1\rangle + \gamma_2 |2\rangle \tag{19}$$

of a single-mode light field which is an arbitrary superposition of vacuum, one and two photon states. Such a state may be prepared using a quantum scissors device described in [7]. Our gedankenexperiment uses ideal photon counters which are able to carry out the von Neumann projection at least onto state $|1\rangle$ [8].

The transmission scheme is depicted in Fig. 6. It consists of two beam splitters BS_1 and BS_2 with equal reflection coefficients r and transmission coefficients t taken to be real (we have $r^2 + t^2 = 1$). 1, 2; a, b, c and A, B refer to different spatial modes, while $\hat{a}_i$ is the annihilation operator of the mode i. As it will be shown later it is important that the beam splitters are "opposed", that is the relationship between modes 1, 2 and b, c is the same as the relationship between modes b, a and B, A respectively:

$$\hat{a}_b = t\hat{a}_2 + r\hat{a}_1, \quad \hat{a}_c = -r\hat{a}_2 + t\hat{a}_1, \tag{20}$$

and

$$\hat{a}_A = t\hat{a}_b - r\hat{a}_a, \quad \hat{a}_B = r\hat{a}_b + t\hat{a}_a. \tag{21}$$

Thus our aim is to teleport a pure state $|\Psi_{\text{in}}\rangle$ of mode a to mode c.

BS_2 is responsible for entangling modes 1 and 2 to provide us with the entangled resource in modes b and c. The states of modes 1 and 2 have to be prepared to be in odd Schrödinger-cat states

$$|\Psi\rangle_1 = |x, -\rangle\,, \tag{22}$$
$$|\Psi\rangle_2 = |ix, -\rangle\,, \tag{23}$$

where x is a real number. These states interfere at BS_2 which, according to Eqs. (20), results in the entangled state

$$|\Psi\rangle_{bc} = \frac{1}{2\left(1 - \mathrm{e}^{-2x^2}\right)} \left(|\alpha\rangle_b |-i\alpha\rangle_c - |\alpha^*\rangle_b |i\alpha^*\rangle_c - |-\alpha^*\rangle_b |-i\alpha^*\rangle_c + |-\alpha\rangle_b |i\alpha\rangle_c\right), \tag{24}$$

where

$$\alpha = (r + it)x \tag{25}$$

has been introduced.

Now modes A and B are subjected to a photon counting measurement. The scheme is *conditional*: the result is accepted if and only if exactly one photon is detected at each detector in coincidence. The probability of this event will be calculated later. The classical information concerning success or failure of the process is communicated to Bob via a classical channel. The successful event is modeled as a von Neumann projective measurement onto $|1\rangle_A |1\rangle_B$. In what follows we suppose that the process was successful. The situation after the measurement is shown in Fig. 7. In modes A and B there are one photon states, so using the inverse of Eqs. (21) we obtain the state of modes a and b after the measurement:

$$|\Psi'\rangle_{ab} = \sqrt{2}rt \left(|0\rangle_a |2\rangle_b - |2\rangle_a |0\rangle_b\right) + (t^2 - r^2) |1\rangle_a |1\rangle_b\,. \tag{26}$$

This is the state the measurement projects the state of modes a and b onto, so after the measurement the state of mode c reads:

$$\begin{aligned} |\Psi_{\text{out}}\rangle &= \frac{1}{\sqrt{\mathcal{P}}} \langle\Psi'|_{ab} \left(|\Psi_{\text{in}}\rangle \otimes |\Psi\rangle_{bc}\right) \\ &= \frac{1}{\sqrt{\mathcal{P}}} \left(\sqrt{2}rt \left(\gamma_0 \langle 2|_b - \gamma_2 \langle 0|_b\right) + (t^2 - r^2)\gamma_1 \langle 1|_b\right) |\Psi\rangle_{bc}\,, \end{aligned} \tag{27}$$

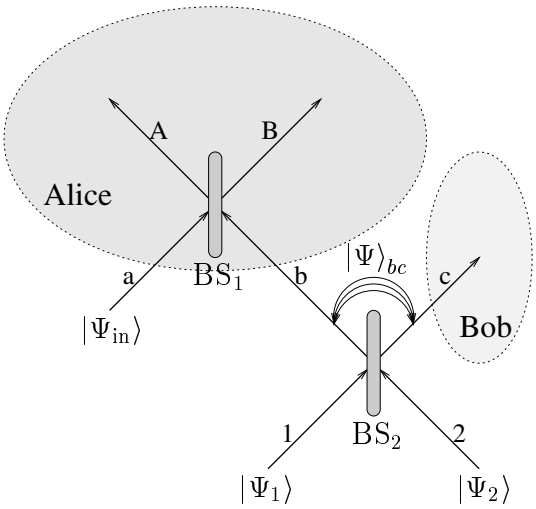

Fig. 6 Scheme for teleportation by means of Schrödinger cats with the states of modes before Alice's measurement.

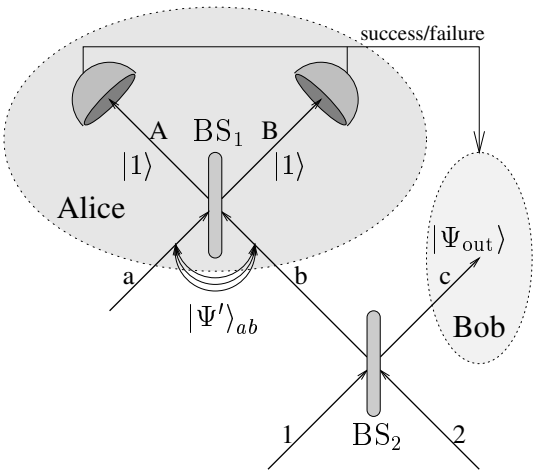

Fig. 7 Scheme with the states after Alice's measurement.

where $\mathcal{P}$ is a normalization factor arising from the projection, and exactly this gives the probability of measuring $|1\rangle_A |1\rangle_B$:

$$\mathcal{P} = \left\| \langle \Psi' |_{ab} \left(|\Psi_{\text{in}}\rangle \otimes |\Psi\rangle_{bc} \right) \right\|^2 \tag{28}$$

The fidelity of the teleportation of a given input state is

$$\mathcal{F} = |\langle \Psi_{\text{in}} | \Psi_{\text{out}} \rangle| \,. \tag{29}$$

The probability of successful measurement and the fidelity may be regarded as a function of x and r in our case. The shape of the functions will depend on the choice of the input state (19). In Fig. 8 for instance, we see the probability of success and the fidelity in the case of $\gamma_0 = \gamma_1 = \gamma_2 = \frac{1}{\sqrt{3}}$, while in Figs. 9–12 for some other simple choices for the input state.

There is an interesting feature, however, which turns out to be independent of the choice of the input state: in the limit of $x \to 0$ there are always two values $r = 0.46$ and $r = 0.89$ where the fidelity is unity, that is, the teleportation is perfect. This can be understood as follows: in the limit of $x \to 0$ the (24) entangled state shared by Alice and Bob becomes

$$|\Psi\rangle_{bc} (x \to 0) = i \left(\sqrt{2} r t (|0\rangle_b |2\rangle_c - |2\rangle_b |0\rangle_c) + (t^2 - r^2) |1\rangle_b |1\rangle_c \right), \tag{30}$$

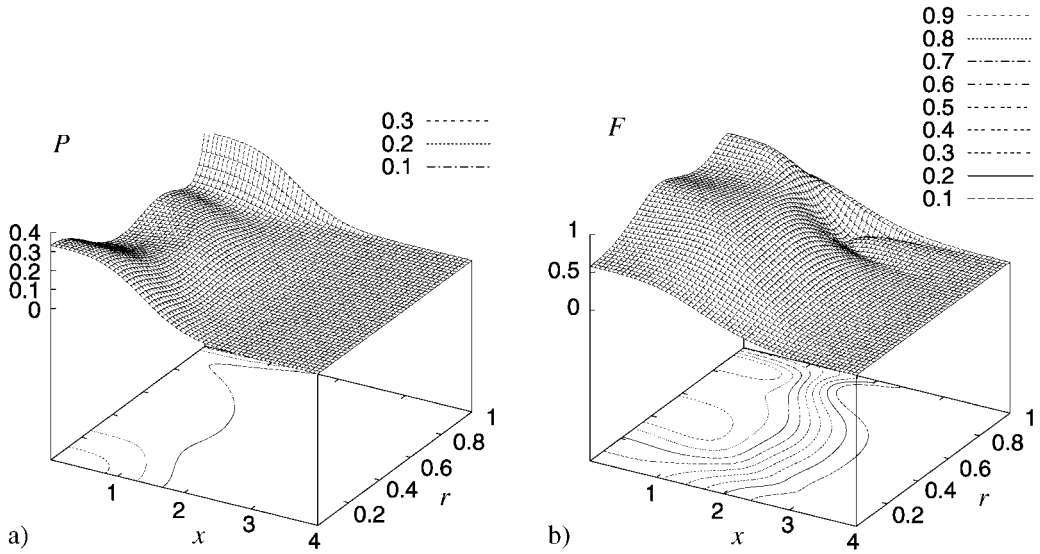

Fig. 8 Probability $\mathcal{P}$ of measuring $|1\rangle_A |1\rangle_B$ and fidelity $\mathcal{F}$ of the scheme for $|\Psi_{\text{in}}\rangle = \frac{1}{\sqrt{3}}(|0\rangle + |1\rangle + |2\rangle)$ as a function of x and r. As $x \to 0$ there are two values $r = 0.46$ and $r = 0.79$ with fidelity 1.

the same state as (26) up to a phase factor. Now, this state becomes maximally entangled when

$$\sqrt{2}rt = t^2 - r^2 \tag{31}$$

that gives $r = 0.46$ and $r = 0.89$. In this case the state that Alice and Bob share is a perfect EPR-pair in the subspace $\{|0\rangle, |1\rangle, |2\rangle\}$, and Alice's one photon measurement is a projection onto a Bell-state of this subspace, so the teleportation of states in this subspace is perfect, i.e. fidelity is 1.

Another interesting feature arising in this scheme is that when the input state is an arbitrary superposition of $|0\rangle$ and $|2\rangle$, fidelity is unity for $x \to 0$ at whatever choice of r. Following the above argument it is easy to understand, because the states (26) and (30) are maximally entangled in the subspace $\{|0\rangle, |2\rangle\}$ independently of r.

6 Further generalization: teleportation of two qubits

We have already shown that the entanglement of the $|g, 2-\rangle$ two-mode SC approaches 2 ebits for large coherent amplitudes. With a proper setup, this may allow the teleportation of states in the appropriate four-dimensional subspace, hence the transmission of two qubits. In the previous section we have given a realistic proposal for transmitting an arbitrary superposition of three states. In the present section we propose a protocol for a two-qubit teleportation that, however, lacks the good experimental prospects of the former.

The teleportation scheme utilizes a $|g, 2-\rangle$ two-mode SC state as the EPR state for the protocol. This state can be generated from two ordinary SC states, $|x, -\rangle$ and $|iy, -\rangle$, by a 50%-50% real beam splitter (BS_2). Unfortunately, this EPR state is never maximally entangled. The possibility of making successful teleportation does not elude, however. With appropriate selection of Alice's measurement, perfect transmission of the input state can be achieved [9]. On the other hand, however, the teleportation becomes conditional.

For putting the general theory to work, we have chosen to parametrize all possible conjugate linear maps as a product of a linear map and the *conjugate* linear map $\mathcal{I}$ defined on the coherent states as $\mathcal{I}|\alpha\rangle = |\alpha^*\rangle$. This selection is rather convenient if we choose to work in the $\mathcal{C} = \{|g\rangle, |g^*\rangle, |-g\rangle, |-g^*\rangle\}$ non-orthogonal

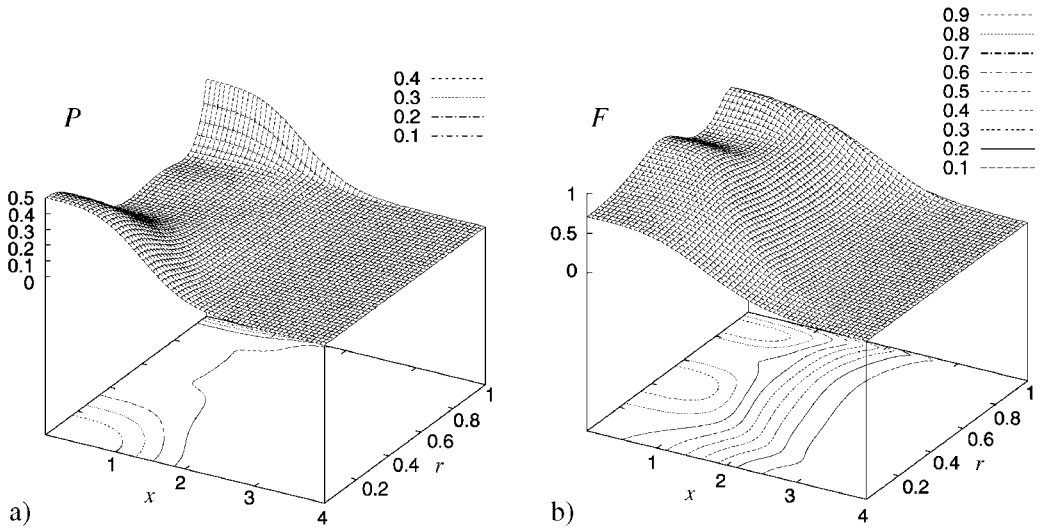

Fig. 9 Probability $\mathcal{P}$ of measuring $|1\rangle_A\,|1\rangle_B$ and fidelity $\mathcal{F}$ of the scheme for $|\Psi_{\text{in}}\rangle = \frac{1}{\sqrt{3}}(|0\rangle + |1\rangle)$ as a function of x and r. As $x \to 0$ there are two values $r = 0.46$ and $r = 0.79$ with fidelity 1.

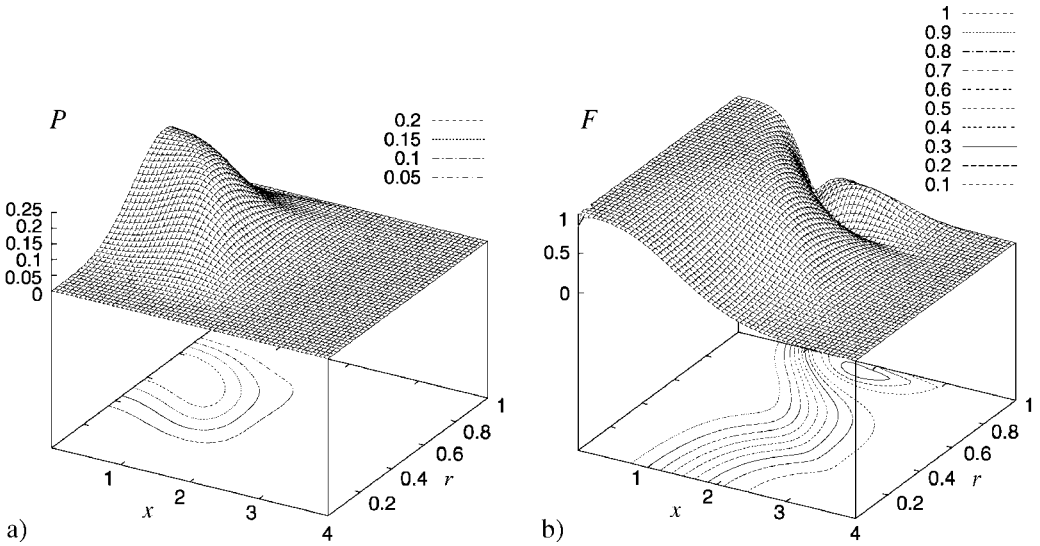

Fig. 10 Probability $\mathcal{P}$ of measuring $|1\rangle_A\,|1\rangle_B$ and fidelity $\mathcal{F}$ of the scheme for $|\Psi_{\text{in}}\rangle = \frac{1}{\sqrt{3}}(|0\rangle + |2\rangle)$ as a function of x and r. As $x \to 0$ fidelity yields constant 1.

basis. We represent the unknown input state as the four dimensional complex vector $\mathbf{A}$, and the EPR state by the 4×4 matrix

$$\mathbf{C}\mathcal{I} = \begin{pmatrix} 1 & 0 & 0 & 0 \\ 0 & -1 & 0 & 0 \\ 0 & 0 & 1 & 0 \\ 0 & 0 & 0 & -1 \end{pmatrix} \begin{pmatrix} 0\,1\,0\,0 \\ 1\,0\,0\,0 \\ 0\,0\,0\,1 \\ 0\,0\,1\,0 \end{pmatrix} = \begin{pmatrix} 0 & 1 & 0 & 0 \\ -1 & 0 & 0 & 0 \\ 0 & 0 & 0 & 1 \\ 0 & 0 & -1 & 0 \end{pmatrix}. \tag{32}$$

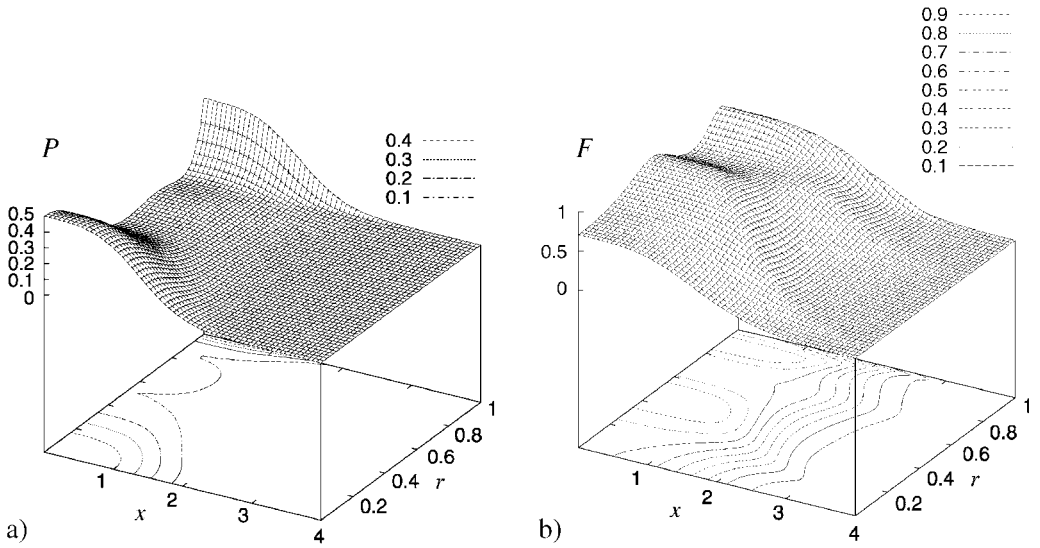

Fig. 11 Probability $\mathcal{P}$ of measuring $|1\rangle_A |1\rangle_B$ and fidelity $\mathcal{F}$ of the scheme for $|\Psi_{\rm in}\rangle = \frac{1}{\sqrt{3}}(|1\rangle + |2\rangle)$ as a function of x and r. As $x \to 0$ there are two values $r = 0.46$ and $r = 0.79$ with fidelity 1.

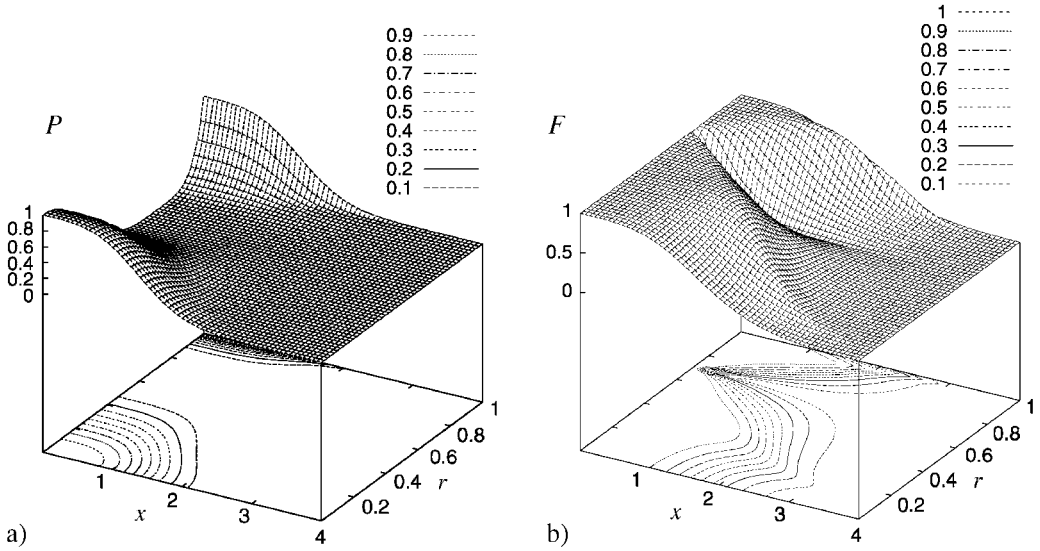

Fig. 12 Probability $\mathcal{P}$ of measuring $|1\rangle_A |1\rangle_B$ and fidelity $\mathcal{F}$ of the scheme for $|\Psi_{\rm in}\rangle = \frac{1}{\sqrt{3}}(|1\rangle)$ as a function of x and r.

Let the quasi-Bell state be written as $|\mathrm{Bell}\rangle = \sum_{i,j=1}^{4} B_{ij} |i\rangle |j\rangle$ (where $|i\rangle$ is the i-th element of basis $\mathcal{C}$). We carry out the calculation for the B matrix in the same manner as for the eigenvalues of the EPR state. With the notation of the Appendix, the result can be written $\mathbf{B} = (\mathbf{G}^T \mathcal{I} \mathbf{C} \mathbf{G})^{-1}$, where $\mathbf{G}^T$ denotes the (real) transpose of $\mathbf{G}$. This formula can be evaluated analytically. In the general case, the resulting matrix contains 8 non-zero terms, hence accounting for 8 terms in the coherent-state expansion. The number of non-zero elements, however, can be reduced to 4 if we require the restriction

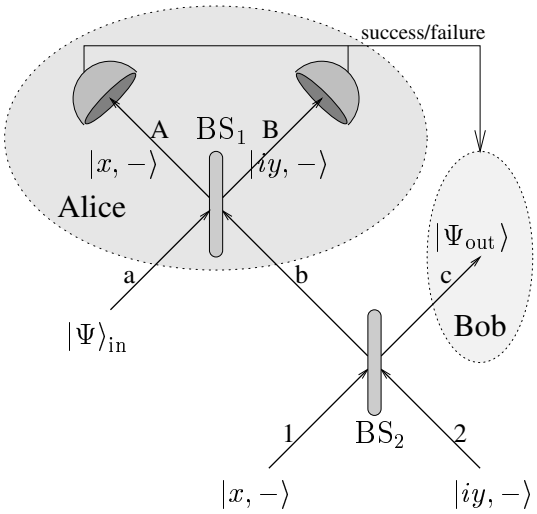

Fig. 13 Teleportation scheme for two qubits.

$$\cos 4\mathbf{Re}g\mathbf{Im}g = 1. \tag{33}$$

This four-term quasi-Bell state then constitutes exactly the same two-mode SC state that is used for the EPR pair. Another restriction $\cos(2\mathbf{Re}g\mathbf{Im}g) = 1$ that includes (33), allows a definition of a simple orthogonal basis. These four basis states are even and odd superpositions of two even (odd) SC states:

$$|g,+\rangle \pm |g^*,+\rangle \quad \text{and} \quad |g,-\rangle \pm |g^*,-\rangle\,. \tag{34}$$

A possible way to project onto the $|\mathrm{Bell}\rangle$ quasi-Bell state is to use BS_1 beam splitter with the same parameters as BS_2. For proper results, however, the input ports of BS_1 must be chosen such that they correspond to the output ports of BS_2. That is, the beam splitters must be used facing each other. Notice the similarity of the current setup and that of section 5. In this case, however, the measurement that is to be performed is more complicated. For an arbitrary input state, the states of modes A, B and c are

$$\begin{aligned}
&|0\rangle_A\,|...\rangle_B\,|...\rangle_c + |\ldots\rangle_A\,|0\rangle_B\,|...\rangle_c \\
&+1/4\,|x,+\rangle_A\,|iy,+\rangle_B\,(-A_1\,|g\rangle + A_2\,|g^*\rangle - A_3\,|-g\rangle + A_4\,|-g^*\rangle)_c \\
&+1/4\,|x,-\rangle_A\,|iy,+\rangle_B\,(-A_1\,|g\rangle + A_2\,|g^*\rangle + A_3\,|-g\rangle - A_4\,|-g^*\rangle)_c \\
&+1/4\,|x,+\rangle_A\,|iy,-\rangle_B\,(-A_1\,|g\rangle - A_2\,|g^*\rangle + A_3\,|-g\rangle + A_4\,|-g^*\rangle)_c \\
&+1/4\,|x,-\rangle_A\,|iy,-\rangle_B\,(-A_1\,|g\rangle - A_2\,|g^*\rangle - A_3\,|-g\rangle - A_4\,|-g^*\rangle)_c \\
&+1/4\,|iy,+\rangle_A\,|x,+\rangle_B\,(-A_1\,|-g\rangle + A_2\,|-g^*\rangle - A_3\,|g\rangle + A_4\,|g^*\rangle)_c \\
&+1/4\,|iy,+\rangle_A\,|x,-\rangle_B\,(-A_1\,|-g\rangle + A_2\,|-g^*\rangle + A_3\,|g\rangle - A_4\,|g^*\rangle)_c \\
&+1/4\,|iy,-\rangle_A\,|x,+\rangle_B\,(-A_1\,|-g\rangle - A_2\,|-g^*\rangle + A_3\,|g\rangle + A_4\,|g^*\rangle)_c \\
&+1/4\,|iy,-\rangle_A\,|x,-\rangle_B\,(-A_1\,|-g\rangle - A_2\,|-g^*\rangle - A_3\,|g\rangle - A_4\,|g^*\rangle)_c
\end{aligned} \tag{35}$$

before the measurement. (We have introduced $g = (x+iy)/\sqrt{2}$ for simplicity.) Since five states appear in the expansion in each modes, to project onto the desired quasi-Bell state, we need special detectors projecting onto the Schrödinger cat states $|x,-\rangle$ and $|iy,-\rangle$. This can only be performed by detectors those have the ability to distinguish $|x,-\rangle$, $|iy,-\rangle$ from the vacuum ($|0\rangle$) and $|x,+\rangle$, $|iy,+\rangle$, and in addition, also from each other. Notice, that in the present case, a simple detector able to detect the presence of exactly one photon is not sufficient, since both odd SC states contain $|1\rangle$ although with different coefficients. One possibility could be to divert the beam proportional to the modulus of its coherent amplitude, and then performing a measurement discriminating between even and odd number of photons. The only backset

of this method is that, not also it requires very fine setting of two different coherent pulses, but also high coherent amplitudes. Whereas, at such high intensities, the used Schrödinger cats become rather prone to decoherence.

7 Conclusions

Two-mode entangled optical Schrödinger cat states obtained by mixing one-mode Schrödinger cats on a beam splitter were considered. A formal description of the states was given in terms of the photon number expansion and the time-dependent wavefunction. The entanglement of these states was quantified using a nonorthogonal basis for the calculations. For small separation of the component coherent states the two-mode entangled Schrödinger cat states are similar to two-mode amplitude squeezed vacua.

The entanglement of the states allows them to be used for quantum teleportation, a very important primitive of quantum communication. Two quantum teleportation schemes with two-mode entangled Schrödinger cats playing the role of the EPR pair were considered. It was shown that arbitrary superpositions of the $|0\rangle$, $|1\rangle$, and $|2\rangle$ Fock states can be conditionally teleported by two-mode Schrödinger cats. The fidelity of the teleportation has been shown to reach 1 for modified Schrödinger cats in certain limiting cases. As a generalization of this protocol, it has been demonstrated how can two qubits be teleported at once using only one entangled resource. Although this scheme is experimentally less feasible, is shows the maximum capabilities of the two-mode Schrödinger cat state.

A Calculating entropy and entanglement in a non-orthogonal basis

A.1 Non-orthogonal basis

A set of N linearly independent vectors of a Hilbert space, $B := \{|i\rangle \in \mathcal{H} | i \ < N\}$ span a Hilbert space of N dimensions: $\mathcal{H}' := \mathrm{Span}\, B$.

Elements of the Hilbert space $\mathcal{H}'$ and linear operators with support and range in $\mathcal{H}'$ can be represented by vectors and matrices in the usual way: $|x\rangle = \sum_i x_i |i\rangle$, $\hat{A} = \sum_{ij} A_{ij} |i\rangle \langle j|$.

With the introduction of the metric tensor $G_{ij} := \langle i | j \rangle$, the scalar product of two vectors can be given as a compact formula:

$$\langle x | y \rangle = \sum_{ij} x_i^* y_j \langle i | j \rangle = \mathbf{x}^* \mathbf{G} \mathbf{y}.$$

We can use the same representation if we want to calculate the effect of the operator $\hat{A}$ on a vector $|x\rangle \in \mathcal{H}'$. Let $|y\rangle = \hat{A} |x\rangle$, then the following equation holds:

$$\mathbf{y} = \mathbf{A}\mathbf{G}\mathbf{x}.$$

It follows that the eigenvalue problem $\hat{A} |x\rangle = \lambda |x\rangle$ for the linear operator $\hat{A}$, using our non-orthogonal representation introduced above, can be written as:

$$(\mathbf{A}\mathbf{G})\, \mathbf{x} = \lambda \mathbf{x}.$$

This means that the eigenvalues of the linear operator $\hat{A}$ are the same as those of the matrix $\mathbf{AG}$, and the eigenvectors of the first are represented by the eigenvectors of the second.

A.2 Calculating entropies

Let us take a bipartite quantum system with Hilbert space $\mathcal{H} = \mathcal{H}_a \otimes \mathcal{H}_b$, and finite sets of linearly independent states in the two component spaces: $B_a := \{|i\rangle_a \in \mathcal{H}_a | i \ < N_a\}$, $B_b := \{|j\rangle_b \in \mathcal{H}_b | j \ < N_b\}$, with metric tensors $G^{(a)}_{ik} = {}_a\langle i | k \rangle_a$, and $G^{(b)}_{jl} = {}_b\langle j | l \rangle_b$.

Let $|\psi\rangle$ be a pure state of the bipartite quantum system that can be expanded in the following way:

$$|\psi\rangle = \sum_{i=0}^{N_a} \sum_{j=0}^{N_b} \psi_{ij} \, |i\rangle_a \, |j\rangle_b \, .$$

Its density operator is

$$\hat{\varrho} = \sum_{i,k=0}^{N_a} \sum_{j,l=0}^{N_b} \psi_{ij} \psi_{kl}^* \, |i\rangle_a \, |j\rangle_b \, {}_a\langle k| {}_b\langle l| \, .$$

The reduced density operator of system a is formed by tracing over system b:

$$\hat{\varrho}^{(a)} := \mathrm{Tr}_b\{\hat{\varrho}\} = \sum_{i,k=0}^{N_a} \left(\sum_{j,l=0}^{N_b} \psi_{ij} \psi_{kl}^* G_{lj}^{(b)} \right) |i\rangle_a \, {}_a\langle k|$$

We can see that the matrix representing the density operator $\hat{\varrho}^{(a)}$ in the non-orthogonal basis of system a is:

$$\varrho_{ij}^{(a)} := \sum_{k,l=0}^{N_b} \psi_{ik} \psi_{jl}^* G_{lk}^{(b)} \, .$$

Suppose we want to calculate the *entanglement* of $|\psi\rangle$, i.e. the entropy of subsystem a:

$$S^{(a)} = -k_B \, \mathrm{Tr}_a(\hat{\varrho}^{(a)} \ln \hat{\varrho}^{(a)}) = -k_B \Sigma_i \lambda_i^{(a)} \ln \lambda_i^{(a)},$$

where the $\lambda_i^{(a)}$'s are the eigenvalues of $\hat{\varrho}^{(a)}$. Using the non-orthogonal basis of system a, the eigenvalues of $\hat{\rho}^{(a)}$ are therefore the eigenvalues of the $(N_a \times N_a)$ matrix

$$\sum_{m=0}^{N_a} \sum_{k,l=0}^{N_b} \psi_{ik} \psi_{ml}^* G_{lk}^{(b)} G_{mj}^{(a)}.$$

These eigenvalues can then be determined numerically or analytically.

References

[1] P. Domokos and J. Janszky, Phys. Lett. A **186**, 289 (1994).
[2] Chin-lin Chai, Phys. Rev. A **46**, 7187 (1992).
[3] S. J. van Enk and O. Hirota, Phys. Rev. A **64**, 022313 (2001).
[4] H. Jeong, M. S. Kim, and Jinhyoung Lee, Phys. Rev. A **64**, 052308-1 (2001).
[5] S. M. Barnett and S. J. D. Phoenix, Phys. Rev. A **40**, 2404 (1989).
[6] C. M. Caves, C. Zhu, G. J. Milburn, and W. Schleich, Phys. Rev. A **43**, 3854 (1991).
[7] M. Koniorczyk, Z. Kurucz, A. Gábris, and J. Janszky, Phys. Rev. A **62**, 013802 (2000).
[8] H. Paul, P. Törmä, T. Kiss, and I. Jex, Phys. Rev. Lett. **76**, 2464 (1996).
[9] Z. Kurucz, M. Koniorczyk, and J. Janszky, Fortschr. Phys. **49**, 1019 (2001).